
Proceedings Paper:
Zhang, J. and Liu, W. (2022) Antenna selection design of crossed-dipole arrays for multi-beam multiplexing based on a hybrid beamforming structure. In: 2022 IEEE International Symposium on Circuits and Systems (ISCAS). 2022 IEEE International Symposium on Circuits and Systems (ISCAS), 27 May - 01 Jun 2022, Austin, TX, USA. IEEE, pp. 2604-2608. ISBN: 978-1-6654-8486-2. ISSN: 0271-4302. EISSN: 2158-1525.

https://doi.org/10.1109/iscas48785.2022.9937860

Antenna Selection Design of Crossed-Dipole Arrays for Multi-Beam Multiplexing Based on a Hybrid Beamforming Structure

Junwei Zhang and Wei Liu
Department of Electronic and Electrical Engineering
University of Sheffield, S1 3JD, UK

***Abstract*—Multi-beam multiplexing design based on the interleaved subarray architecture can be achieved by uniform linear arrays (ULAs) consisting of isotropic antennas in previous works. By considering the polarisation information of a signal, the crossed-dipole array is employed, where each antenna is associated with two complex-valued weighting coefficients. To reduce the implementation complexity of the system, when a large number of crossed-dipole antennas are available, we may not need to employ all of them and a subset of the available antennas may be sufficient for a specific beamforming scenario. For this purpose, two design methods are proposed to select the best set of crossed-dipole antennas or dipoles. Designed examples are provided to verify the effectiveness of the proposed methods.**

***Index Terms*—Antenna selection, crossed-dipole array, multi-beam multiplexing, hybrid beamforming.**

I. Introduction

As a widely recognised solution for the implementation of massive MIMO and mmWave communications in 5G and beyond [1]–[12], the hybrid beamforming scheme combines the analogue beamforming technique [13]–[15], and the digital one together [16]. One representative hybrid beamforming architecture is the sub-aperture based hybrid beamformer [4], [6], [17], [18], and there are mainly two types of them: one is the side-by-side type or localised subarray architecture and the other one is the interleaved architecture [19]–[23].

Recently, a hybrid beamforming method which involves multiplexing multiple beams was proposed [24], [25]. One particular feature of the above methods is that, the number of analogue coefficients is the same as the number of antennas, independent of the number of beams generated, while the number of subarrays is the same as the number of beams.

However, in the above multi-beam multiplexing designs based on the interleaved subarray architecture, the polarisation information of the signals has not been considered yet. In this work, we exploit the polarisation information in the design by replacing the isotropic antennas in the structure with the polarisation-sensitive crossed-dipole antennas. Each antenna in the crossed-dipole array consists of two orthogonally orientated dipoles which can measure both the horizontal and vertical components of a received signal [26]–[29]. Similar to [30], we consider a low-complexity implementation problem, i.e., when a large number of crossed-dipole antennas are available, we may not need to employ all of them and a subset of the available antennas may be sufficient for a specific beamforming scenario. For this purpose, in addition to the usual beamforming constraints, we also consider minimising the coefficients associated with the antennas so that those antennas with small enough weighting coefficients can be switched off for a particular beamforming scenario. Different from the isotropic antenna case considered in [30], for crossed-dipole antennas, there are two complex-valued weighting coefficients associated with each antenna [31]–[34] and therefore we have two choices: either switch off the whole crossed-dipole antenna or one of the dipoles. To implement these two different implementation schemes, two corresponding compressive sensing (CS) based design methods are proposed. Design examples are provided, which show that performance of the scheme for switching off the whole crossed-dipole antenna is not as good as the case for switching off individual dipoles due to more constraints imposed on the design.

For the remaining part, a review of the interleaved architecture and the crossed-dipole array is presented in Sec. II; the proposed design is described in Sec. III; design examples are provided in Sec. IV and conclusions drawn in Sec. V.

II. Array Model

The interleaved subarray architecture based on an N-element ULA is shown in Fig. 1, where the adjacent antenna spacing is d. Suppose the N antennas of the ULA are split into M interleaved subarrays. Then, each subarray consists of $N_{\rm s} = N/M$ antennas with an adjacent antenna spacing $d_m = Md$. The phase shift between adjacent subarrays is $e^{j2\pi\frac{d}{\lambda}sin\theta}$, where the direction of angle θ is measured from the broadside.

Without loss of generality, consider the case of $M = 2$. Each of the two linear crossed-dipole subarrays with $N_{\rm s}$ antennas is shown in Fig. 2, where each antenna consists of two orthogonally orientated dipoles, and the complex-valued weighting coefficients parallel to the x-axis and y-

This work is supported by the UK Engineering and Physical Sciences Research Council (EPSRC) under grants EP/T517215/1 and EP/V009419/1.

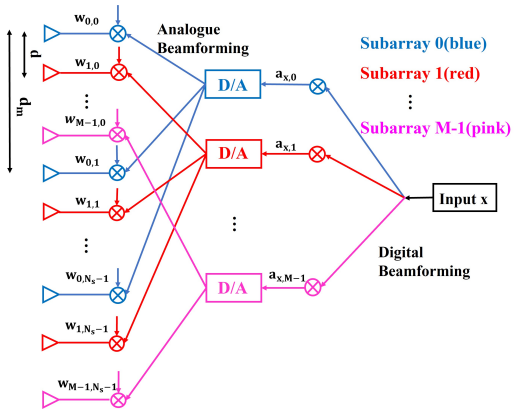

Fig. 1. An interleaved subarray based hybrid beamforming structure.

axis are $w_{\mathrm{n,x}}$ and $w_{\mathrm{n,y}}$, respectively, for $n = 0, 1, ..., N_{\mathrm{s}} - 1$. In addition, the elevation and azimuth angles are given by $\theta \in [-\frac{\pi}{2}, \frac{\pi}{2}]$ and $\phi \in [-\pi, \pi]$, respectively [31], [35].

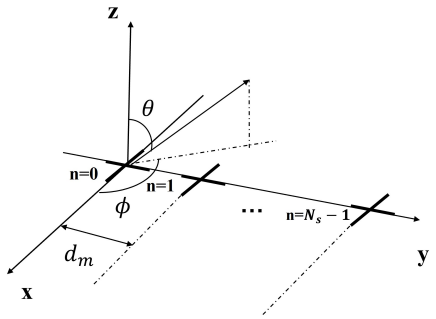

Fig. 2. A linear crossed-dipole array

The spatial steering vector of the m-th subarray with the interleaved subarray architecture is given by

$$\begin{aligned}\mathbf{s}_{\mathrm{m,s}}(\theta,\phi) =&[e^{j2\pi m\frac{d}{\lambda}\sin\theta\sin\phi}, e^{j2\pi(m+M)\frac{d}{\lambda}\sin\theta\sin\phi},\\ &..., e^{j2\pi(m+M(N_{\mathrm{s}}-1))\frac{d}{\lambda}\sin\theta\sin\phi}]^{\mathrm{T}},\end{aligned} \tag{1}$$

where $[.]^{\mathrm{T}}$ denotes the transpose operation with $m \in \{0, 1\}$. Moreover, the spatial-polarisation coherent vector consisting of a signal's polarisation information is

$$\mathrm{s_p}(\theta,\phi,\sigma,\eta) = \begin{bmatrix}\sin\sigma\cos\theta\cos\phi e^{j\eta} - \cos\sigma\sin\phi\\ \sin\sigma\cos\theta\sin\phi e^{j\eta} + \cos\sigma\cos\phi\end{bmatrix} = \begin{bmatrix}s_{\mathrm{p,x}}(\theta,\phi,\sigma,\eta)\\ s_{\mathrm{p,y}}(\theta,\phi,\sigma,\eta)\end{bmatrix}, \tag{2}$$

where $\sigma \in [0, \frac{\pi}{2}]$ is the auxiliary angle and $\eta \in [-\pi, \pi)$ is the polarisation phase difference.

The m-th subarray can be split into two parts and each parallel to the corresponding axis. With $f \in \{x, y\}$, the steering vector of each part for the m-th subarray is

$$\mathbf{s}_{\mathrm{m,f}}(\theta,\phi,\sigma,\eta) = \mathrm{s_{p,f}}(\theta,\phi,\sigma,\eta)\mathbf{s}_{\mathrm{m,s}}(\theta,\phi). \tag{3}$$

The beam pattern generated by the m-th subarray is

$$P_{\mathrm{m}}(\theta,\phi,\sigma,\eta) = \mathbf{w}_{\mathrm{A,m}}^{\mathrm{H}}\mathbf{s}_{\mathrm{m}}(\theta,\phi,\sigma,\eta), \tag{4}$$

where $[.]^{\mathrm{H}}$ denotes the Hermitian transpose and $\mathbf{w}_{\mathrm{A,m}}$ denotes the analogue coefficients for the m-th subarray, given by

$$\mathbf{w}_{\mathrm{A,m}} = [w_{\mathrm{A,m,x},0}, w_{\mathrm{A,m,y},0}, w_{\mathrm{A,m,x},1}, ..., w_{\mathrm{A,m,y,N_s}-1}]^{\mathrm{T}}, \tag{5}$$

where $w_{\mathrm{A,m,f,n}}$ is the complex weighting coefficient for the n-th dipole parallel to the f-axis. Similarly,

$$\begin{aligned}\mathbf{s}_{\mathrm{m}}(\theta,\phi,\sigma,\eta) = [&s_{\mathrm{m,x},0}(\theta,\phi,\sigma,\eta), s_{\mathrm{m,y},0}(\theta,\phi,\sigma,\eta),\\ &s_{\mathrm{m,x},1}(\theta,\phi,\sigma,\eta), \ldots, s_{\mathrm{m,y,N_s}-1}(\theta,\phi,\sigma,\eta)]^{\mathrm{T}},\end{aligned} \tag{6}$$

where $s_{\mathrm{m,f,n}}(\theta,\phi,\sigma,\eta)$ is the contribution of the n-th dipole in the m-th subarray to the overall steering vector parallel to the f-axis.

The digital coefficient vector for the k-th designed beam is given by $\mathbf{w}_{\mathrm{D,k}} = [a_{\mathrm{k},0}, a_{\mathrm{k},1}]$ with $k \in \{0, 1\}$. So the designed beam pattern for the beam in direction φ_{k} is

$$\begin{aligned}P_{\varphi_{\mathrm{k}}}(\theta,\phi,\sigma,\eta) &= a_{\mathrm{k},0}^{*}P_0(\theta,\phi,\sigma,\eta) + a_{\mathrm{k},1}^{*}P_1(\theta,\phi,\sigma,\eta)\\ &= a_{\mathrm{k},0}^{*}\mathbf{w}_{\mathrm{A},0}^{\mathrm{H}}\mathbf{s}_0(\theta,\phi,\sigma,\eta) + a_{\mathrm{k},1}^{*}\mathbf{w}_{\mathrm{A},1}^{\mathrm{H}}\mathbf{s}_1(\theta,\phi,\sigma,\eta),\end{aligned} \tag{7}$$

where $*$ denotes the conjugate operation.

III. The Proposed Designs

The problem considered in this work can be stated as follows: when there are a large number of antennas available in a massive MIMO system, for a particular beamforming scenario, we may not need to employ all of them and only a subset of the antenna channels are required; when the beamforming scenario changes, we then find another subset of antennas and this change can be implemented by electronic switching. To find the subset of antennas for a particular scenario, as mentioned earlier, for the crossed-dipole antenna based structure, we have two choices: either choosing to switch off the individual dipoles of each crossed-dipole antenna or switch off the whole crossed-dipole antennas.

A. Switch off individual dipoles

With (7) and $\mathbf{a}_{\mathrm{k,m}} = a_{\mathrm{k,m}}\mathbf{I}_0$, the sum of sidelobe patterns for the two beams is given by

$$\begin{aligned}E_{\mathrm{s}} =& \sum_{\theta\in\Theta_{\mathrm{s}_0}}|P_{\varphi_0}(\theta,\phi,\sigma,\eta)|^2 + \sum_{\theta\in\Theta_{\mathrm{s}_1}}|P_{\varphi_1}(\theta,\phi,\sigma,\eta)|^2\\ =&\mathbf{w}_{\mathrm{A},0}^{\mathrm{H}}\left(\mathbf{a}_{0,0}^{\mathrm{H}}\mathbf{Q}_{\mathrm{S00}}\mathbf{a}_{0,0} + \mathbf{a}_{1,0}^{\mathrm{H}}\mathbf{Q}_{\mathrm{S10}}\mathbf{a}_{1,0}\right)\mathbf{w}_{\mathrm{A},0}\\ &+\mathbf{w}_{\mathrm{A},1}^{\mathrm{H}}\left(\mathbf{a}_{0,1}^{\mathrm{H}}\mathbf{Q}_{\mathrm{S01}}\mathbf{a}_{0,1} + \mathbf{a}_{1,1}^{\mathrm{H}}\mathbf{Q}_{\mathrm{S11}}\mathbf{a}_{1,1}\right)\mathbf{w}_{\mathrm{A},1}\\ &+\mathbf{w}_{\mathrm{A},0}^{\mathrm{H}}\left(\mathbf{a}_{0,0}^{\mathrm{H}}\mathbf{P}_{\mathrm{S00}}\mathbf{a}_{0,1} + \mathbf{a}_{1,0}^{\mathrm{H}}\mathbf{P}_{\mathrm{S10}}\mathbf{a}_{1,1}\right)\mathbf{w}_{\mathrm{A},1}\\ &+\mathbf{w}_{\mathrm{A},1}^{\mathrm{H}}\left(\mathbf{a}_{0,1}^{\mathrm{H}}\mathbf{P}_{\mathrm{S01}}\mathbf{a}_{0,0} + \mathbf{a}_{1,1}^{\mathrm{H}}\mathbf{P}_{\mathrm{S11}}\mathbf{a}_{1,0}\right)\mathbf{w}_{\mathrm{A},0}, \text{with}\end{aligned} \tag{8}$$

$$\begin{aligned}\mathbf{Q}_{\mathrm{S_{km}}} &= \sum_{\theta\in\Theta_{\mathrm{s_k}}}\mathbf{s}_{\mathrm{m}}(\theta,\phi,\sigma,\eta)\mathbf{s}_{\mathrm{m}}(\theta,\phi,\sigma,\eta)^{\mathrm{H}},\\ \mathbf{P}_{\mathrm{S_{k0}}} &= \sum_{\theta\in\Theta_{\mathrm{s_k}}}\mathbf{s}_0(\theta,\phi,\sigma,\eta)\mathbf{s}_1(\theta,\phi,\sigma,\eta)^{\mathrm{H}},\\ \mathbf{P}_{\mathrm{S_{k1}}} &= \sum_{\theta\in\Theta_{\mathrm{s_k}}}\mathbf{s}_1(\theta,\phi,\sigma,\eta)\mathbf{s}_0(\theta,\phi,\sigma,\eta)^{\mathrm{H}},\end{aligned} \tag{9}$$

where $\{k, m\} \in \{0, 1\}$, $\mathbf{I}_0$ denotes a $2N_{\mathrm{s}} \times 2N_{\mathrm{s}}$ identity matrix and $\Theta_{\mathrm{s_k}}$ denotes the sidelobe region for the k-th

beam. Combining $\mathbf{w}_{\mathrm{A},0}$ and $\mathbf{w}_{\mathrm{A},1}$ into one vector, given by $\mathbf{w}_{\mathrm{A}} = \left[\mathbf{w}_{\mathrm{A},0}^{\mathrm{T}}, \mathbf{w}_{\mathrm{A},1}^{\mathrm{T}}\right]^{\mathrm{T}}$, (8) can be rewritten as $E_{\mathrm{s}} = \mathbf{w}_{\mathrm{A}}^{\mathrm{H}}(\mathbf{Q}_{\mathrm{S}} + \mathbf{P}_{\mathrm{S}}\tilde{\mathbf{I}}_0)\mathbf{w}_{\mathrm{A}}$, with

$$\mathbf{Q}_{\mathrm{S}} = \mathrm{diag}(\mathbf{G}_{\mathrm{S}_0}, \mathbf{G}_{\mathrm{S}_1}), \mathbf{P}_{\mathrm{S}} = \mathrm{diag}(\mathbf{H}_{\mathrm{S}_0}, \mathbf{H}_{\mathrm{S}_1}), \tilde{\mathbf{I}}_0 = \begin{bmatrix} \mathbf{0}_{2\mathrm{N_s}} & \mathbf{I}_0 \\ \mathbf{I}_0 & \mathbf{0}_{2\mathrm{N_s}} \end{bmatrix}, \tag{10}$$

$$\begin{aligned} \mathbf{G}_{\mathrm{S_m}} &= \mathbf{a}_{0,\mathrm{m}}^{\mathrm{H}}\mathbf{Q}_{\mathrm{S}_{0\mathrm{m}}}\mathbf{a}_{0,\mathrm{m}} + \mathbf{a}_{1,\mathrm{m}}^{\mathrm{H}}\mathbf{Q}_{\mathrm{S}_{1\mathrm{m}}}\mathbf{a}_{1,\mathrm{m}}, \\ \mathbf{H}_{\mathrm{S}_0} &= \mathbf{a}_{0,0}^{\mathrm{H}}\mathbf{P}_{\mathrm{S}_{00}}\mathbf{a}_{0,1} + \mathbf{a}_{1,0}^{\mathrm{H}}\mathbf{P}_{\mathrm{S}_{10}}\mathbf{a}_{1,1}, \\ \mathbf{H}_{\mathrm{S}_1} &= \mathbf{a}_{0,1}^{\mathrm{H}}\mathbf{P}_{\mathrm{S}_{01}}\mathbf{a}_{0,0} + \mathbf{a}_{1,1}^{\mathrm{H}}\mathbf{P}_{\mathrm{S}_{11}}\mathbf{a}_{1,0}, \end{aligned} \tag{11}$$

where $\mathbf{0}_{2\mathrm{N_s}}$ is a $2N_{\mathrm{s}} \times 2N_{\mathrm{s}}$ all-zero vector and diag $(.)$ denotes the diagonalisation operation.

To find the optimum $\mathbf{w}_{\mathrm{A}}$ with minimum number of nonzero-valued coefficients for a given set of $a_{\mathrm{k,m}}(\{k,m\} \in \{0,1\})$, so that those dipoles with zero-valued coefficients can be switched off, the new formulation is given by

$$\begin{aligned} &\min_{\mathbf{w}_{\mathrm{A}}} \quad J_{\mathrm{LSE}} = (1-\alpha) \parallel \mathbf{L}^{\mathrm{H}}\mathbf{w}_{\mathrm{A}} \parallel_2 + \alpha \parallel \mathbf{w}_{\mathrm{A}} \parallel_1, \\ &\text{subject} \quad \text{to} \\ &\mathbf{w}_{\mathrm{A}}^{\mathrm{H}} \begin{bmatrix} \mathbf{a}_{0,0}^{\mathrm{H}}\mathbf{z}_{\mathrm{S}_{00}} & \mathbf{a}_{1,0}^{\mathrm{H}}\mathbf{z}_{\mathrm{S}_{10}} \\ \mathbf{a}_{0,1}^{\mathrm{H}}\mathbf{z}_{\mathrm{S}_{01}} & \mathbf{a}_{1,1}^{\mathrm{H}}\mathbf{z}_{\mathrm{S}_{11}} \end{bmatrix} = \begin{bmatrix} 1 & 1 \end{bmatrix}, \mathbf{z}_{\mathrm{S_{km}}} = \sum_{\theta \in \Theta_{\mathrm{m_k}}} \mathbf{s}_{\mathrm{m}}(\theta, \phi, \sigma, \eta), \end{aligned} \tag{12}$$

where $\alpha \in (0,1)$ is a trade-off factor between the two parts, $\parallel . \parallel_1$ is the l_1 norm, $\Theta_{\mathrm{m_k}}$ denotes the mainlobe region for the k-th beam and $\mathbf{L} = \mathbf{V}\mathbf{U}^{1/2}$, with $\mathbf{U}$ being the diagonal matrix including all the eigenvalues of $(\mathbf{Q}_{\mathrm{S}} + \mathbf{P}_{\mathrm{S}}\tilde{\mathbf{I}}_0)$ and $\mathbf{V}$ being the corresponding eigenvector matrix [36]. The problem in (12) can be solved by the CVX toolbox in [37].

B. Switch off the whole antenna

One issue with the above antenna selection design is that the two complex-valued weighting coefficients associated with each crossed-dipole antenna cannot be minimised simultaneously. As a result, it will result in some of the crossed-dipole antennas being only partially switched off, which may not be convenient in practice depending on the specific design/structure of the antennas.

To switch off the whole antenna, we have to modify the formulation in (12) so that the two complex-valued coefficients for each antenna can be minimised simultaneously. Following the idea in [38], the formulation in (12) can be modified to

$$\begin{aligned} &\min_{\mathbf{w}_{\mathrm{A}}} \quad J_{\mathrm{LSE}} = (1-\alpha) \parallel \mathbf{L}^{\mathrm{H}}\mathbf{w}_{\mathrm{A}} \parallel_2 + \alpha g \quad (g \in \mathbb{R}^+), \\ &\text{subject} \quad \text{to} \quad \sum_{\tilde{n}=0}^{2N_{\mathrm{s}}-1} ||\mathbf{w}_{\mathrm{A}_{\tilde{\mathrm{n}}}}||_2 \leq g, \text{the 1st constraint in (12)}, \end{aligned} \tag{13}$$

where $\mathbf{w}_{\mathrm{A}} = [w_{\mathrm{A,x},0}, w_{\mathrm{A,y},0}, w_{\mathrm{A,x},1}, ..., w_{\mathrm{A,y},2\mathrm{N_s}-1}]^{\mathrm{T}}$ and $\mathbf{w}_{\mathrm{A}_{\tilde{n}}} = [w_{\mathrm{A,x,\tilde{n}}}, w_{\mathrm{A,y,\tilde{n}}}], (\tilde{n} = 0, 1, \ldots, 2N_{\mathrm{s}} - 1)$.

To minimise the combined weighting coefficients for each crossed-dipole separately, g is decomposed into $g = [1, \ldots, 1]\left[g_0, \cdots, g_{2\mathrm{N_s}-1}\right]^{\mathrm{T}} = \mathbf{1}^{\mathrm{T}}\mathbf{g}$ and (13) is changed to

$$\begin{aligned} &\min_{\mathbf{w}_{\mathrm{A}}} \quad J_{\mathrm{LSE}} = (1-\alpha) \parallel \mathbf{L}^{\mathrm{H}}\mathbf{w}_{\mathrm{A}} \parallel_2 + \alpha \mathbf{1}^{\mathrm{T}}\mathbf{g}, \\ &\text{subject} \quad \text{to} \quad \text{the 1st constraint in (12)}, \\ &\qquad\qquad ||\mathbf{w}_{\mathrm{A}_{\tilde{\mathrm{n}}}}||_2 \leq g_{\tilde{\mathrm{n}}}, \tilde{n} = 0, 1, \ldots, 2N_{\mathrm{s}} - 1. \end{aligned} \tag{14}$$

Note that a value of $g_{\tilde{\mathrm{n}}} = 0$ indicates the second constraint in (14) ensures that both the real and imaginary parts of each coefficient in $\mathbf{w}_{\mathrm{A}_{\tilde{\mathrm{n}}}}$ are zero and the sparse nature of antenna locations is introduced.

Now, by defining $\mathbf{I}_1$ is an $N_{\mathrm{s}} \times N_{\mathrm{s}}$ identity matrix,

$$\tilde{\mathbf{s}}_{\mathrm{m}} = \begin{bmatrix} \mathbf{0} & \mathbf{0} \\ \Re(\mathbf{s}_{\mathrm{m,x},0}) & \Im(\mathbf{s}_{\mathrm{m,x},0}) \\ \Re(\mathbf{s}_{\mathrm{m,y},0}) & \Im(\mathbf{s}_{\mathrm{m,y},0}) \\ -\Im(\mathbf{s}_{\mathrm{m,x},0}) & \Re(\mathbf{s}_{\mathrm{m,x},0}) \\ -\Im(\mathbf{s}_{\mathrm{m,y},0}) & \Re(\mathbf{s}_{\mathrm{m,y},0}) \\ \vdots & \vdots \\ \dot{\mathbf{0}} & \dot{\mathbf{0}} \\ \vdots & \vdots \\ -\Im(\mathbf{s}_{\mathrm{m,y,N_s}-1}) & \Re(\mathbf{s}_{\mathrm{m,y,N_s}-1}) \end{bmatrix}, \tilde{\mathbf{a}}_{\mathrm{k,m}} = a_{\mathrm{k,m}}\mathbf{I}_1, \tag{15}$$

$$\tilde{\mathbf{r}}_{\mathrm{km}} = \begin{bmatrix} \mathbf{0} & \mathbf{0} \\ \Re(\tilde{\mathbf{a}}_{\mathrm{k,m}}^{\mathrm{H}}\mathbf{s}_{\mathrm{m,x},0}) & \Im(\tilde{\mathbf{a}}_{\mathrm{k,m}}^{\mathrm{H}}\mathbf{s}_{\mathrm{m,x},0}) \\ \Re(\tilde{\mathbf{a}}_{\mathrm{k,m}}^{\mathrm{H}}\mathbf{s}_{\mathrm{m,y},0}) & \Im(\tilde{\mathbf{a}}_{\mathrm{k,m}}^{\mathrm{H}}\mathbf{s}_{\mathrm{m,y},0}) \\ -\Im(\tilde{\mathbf{a}}_{\mathrm{k,m}}^{\mathrm{H}}\mathbf{s}_{\mathrm{m,x},0}) & \Re(\tilde{\mathbf{a}}_{\mathrm{k,m}}^{\mathrm{H}}\mathbf{s}_{\mathrm{m,x},0}) \\ -\Im(\tilde{\mathbf{a}}_{\mathrm{k,m}}^{\mathrm{H}}\mathbf{s}_{\mathrm{m,y},0}) & \Re(\tilde{\mathbf{a}}_{\mathrm{k,m}}^{\mathrm{H}}\mathbf{s}_{\mathrm{m,y},0}) \\ \vdots & \vdots \\ \dot{\mathbf{0}} & \dot{\mathbf{0}} \\ \vdots & \vdots \\ -\Im(\tilde{\mathbf{a}}_{\mathrm{k,m}}^{\mathrm{H}}\mathbf{s}_{\mathrm{m,y,N_s}-1}) & \Re(\tilde{\mathbf{a}}_{\mathrm{k,m}}^{\mathrm{H}}\mathbf{s}_{\mathrm{m,y,N_s}-1}) \end{bmatrix}, \tag{16}$$

$$\begin{aligned} \tilde{\mathbf{w}}_{\mathrm{A}} =& [g_0, \Re(w_{\mathrm{A,x},0}), \Re(w_{\mathrm{A,y},0}), -\Im(w_{\mathrm{A,x},0}), -\Im(w_{\mathrm{A,y},0}), \\ & g_1, \ldots, g_{2\mathrm{N_s}-1}, \Re(w_{\mathrm{A,x,2N_s}-1}), \ldots, -\Im(w_{\mathrm{A,y,2N_s}-1})]^{\mathrm{T}}, \end{aligned} \tag{17}$$

$$\mathbf{c} = [\overbrace{1,0,0,0,0}^{\tilde{n}=0}, 1, 0, 0, \cdots, \overbrace{1,0,0,0,0}^{\tilde{n}=2N_{\mathrm{s}}-1}]^{\mathrm{T}}, \tag{18}$$

where $\Re(.)$ and $\Im(.)$ denote the real and imaginary components, respectively, (10) and (11) are changed to

$$\tilde{\mathbf{Q}}_{\mathrm{S}} = \mathrm{diag}(\tilde{\mathbf{G}}_{\mathrm{S}_0}, \tilde{\mathbf{G}}_{\mathrm{S}_1}), \tilde{\mathbf{P}}_{\mathrm{S}} = \mathrm{diag}(\tilde{\mathbf{H}}_{\mathrm{S}_0}, \tilde{\mathbf{H}}_{\mathrm{S}_1}), \tilde{\mathbf{I}}_1 = \begin{bmatrix} \mathbf{0}_{5\mathrm{N_s}} & \mathbf{I}_2 \\ \mathbf{I}_2 & \mathbf{0}_{5\mathrm{N_s}} \end{bmatrix}, \tag{19}$$

$$\begin{aligned} \tilde{\mathbf{G}}_{\mathrm{S_m}} &= \sum_{\theta \in \Theta_{\mathrm{s}_0}} \mathbf{r}_{0,\mathrm{m}}\mathbf{r}_{0,\mathrm{m}}^{\mathrm{T}} + \sum_{\theta \in \Theta_{\mathrm{s}_1}} \mathbf{r}_{1,\mathrm{m}}\mathbf{r}_{1,\mathrm{m}}^{\mathrm{T}}, \\ \tilde{\mathbf{H}}_{\mathrm{S}_0} &= \sum_{\theta \in \Theta_{\mathrm{s}_0}} \tilde{\mathbf{r}}_{0,0}\tilde{\mathbf{r}}_{0,1}^{\mathrm{T}} + \sum_{\theta \in \Theta_{\mathrm{s}_1}} \tilde{\mathbf{r}}_{1,0}\tilde{\mathbf{r}}_{1,1}^{\mathrm{T}}, \\ \tilde{\mathbf{H}}_{\mathrm{S}_1} &= \sum_{\theta \in \Theta_{\mathrm{s}_0}} \tilde{\mathbf{r}}_{0,1}\tilde{\mathbf{r}}_{0,0}^{\mathrm{T}} + \sum_{\theta \in \Theta_{\mathrm{s}_1}} \tilde{\mathbf{r}}_{1,1}\tilde{\mathbf{r}}_{1,0}^{\mathrm{T}}, \end{aligned} \tag{20}$$

where $\mathbf{0}_{5\mathrm{N_s}}$ and $\mathbf{I}_2$ are $5N_{\mathrm{s}} \times 5N_{\mathrm{s}}$ all-zero and identity matrices, respectively. Thus, the final formulation changes to

$$\begin{aligned} &\min_{\tilde{\mathbf{w}}_{\mathrm{A}}} \quad J_{\mathrm{LSE}} = (1-\alpha) \parallel \tilde{\mathbf{L}}^{\mathrm{T}}\tilde{\mathbf{w}}_{\mathrm{A}} \parallel_2 + \alpha \mathbf{c}^{\mathrm{T}}\tilde{\mathbf{w}}_{\mathrm{A}}, \\ &\text{subject} \quad \text{to} \quad \tilde{\mathbf{w}}_{\mathrm{A}}^{\mathrm{T}} \begin{bmatrix} \tilde{\mathbf{z}}_{\mathrm{S}_{00}} & \tilde{\mathbf{z}}_{\mathrm{S}_{10}} \\ \tilde{\mathbf{z}}_{\mathrm{S}_{01}} & \tilde{\mathbf{z}}_{\mathrm{S}_{11}} \end{bmatrix} = \begin{bmatrix} 1 & 0 & 1 & 0 \end{bmatrix}, \\ &||\tilde{\mathbf{w}}_{\mathrm{A}_{\tilde{\mathrm{n}}}}||_2 \leq g_{\tilde{\mathrm{n}}}, \tilde{n} = 0, 1, \ldots, 2N_{\mathrm{s}} - 1, \tilde{\mathbf{z}}_{\mathrm{S_{km}}} = \sum_{\theta \in \Theta_{\mathrm{m_k}}} \tilde{\mathbf{r}}_{\mathrm{km}}, \end{aligned} \tag{21}$$

where $\tilde{\mathbf{L}} = \tilde{\mathbf{V}}\tilde{\mathbf{U}}^{1/2}$, with $\tilde{\mathbf{U}}$ being the diagonal matrix including all the eigenvalues of $(\tilde{\mathbf{Q}}_{\mathrm{S}} + \tilde{\mathbf{P}}_{\mathrm{S}}\tilde{\mathbf{I}}_1)$ and $\tilde{\mathbf{V}}$ being the corresponding eigenvector matrix.

C. Overall design

After obtaining $\tilde{\mathbf{w}}_{\mathrm{A}}$ through either (12) or (21), we can obtain the optimum digital coding coefficients as follows.

Combining $\mathbf{w}_{\mathrm{D},0}$ and $\mathbf{w}_{\mathrm{D},1}$ into one vector, given by $\mathbf{w}_{\mathrm{D}} = \left[\mathbf{w}_{\mathrm{D},0}, \mathbf{w}_{\mathrm{D},1}\right]^{\mathrm{T}} = \left[a_{0,0}, a_{0,1}, a_{1,0}, a_{1,1}\right]^{\mathrm{T}}$, (8) can be rewritten as $E_{\mathrm{s}} = \mathbf{w}_{\mathrm{D}}^{\mathrm{H}} \breve{\mathbf{M}}_{\mathrm{S}} \mathbf{w}_{\mathrm{D}}$, with

$$\breve{\mathbf{M}}_{\mathrm{S}} = \breve{\mathbf{Q}}_{\mathrm{S}} + \breve{\mathbf{P}}_{\mathrm{S}} \tilde{\mathbf{I}}_2, \quad \breve{\mathbf{P}}_{\mathrm{S}} = \mathrm{diag}(\breve{\mathbf{H}}_{\mathrm{S}_0}, \breve{\mathbf{H}}_{\mathrm{S}_1}), \quad \tilde{\mathbf{I}}_2 = \begin{bmatrix} 0 & 1 & 0 & 0 \\ 1 & 0 & 0 & 0 \\ 0 & 0 & 0 & 1 \\ 0 & 0 & 1 & 0 \end{bmatrix}, \tag{22}$$

$$\breve{\mathbf{Q}}_{\mathrm{S}} = \mathrm{diag}(\breve{\mathbf{G}}_{\mathrm{S}_{00}}, \breve{\mathbf{G}}_{\mathrm{S}_{01}}, \breve{\mathbf{G}}_{\mathrm{S}_{10}}, \breve{\mathbf{G}}_{\mathrm{S}_{11}}), \breve{\mathbf{H}}_{\mathrm{S_k}} = \mathrm{diag}(\breve{\mathbf{B}}_{\mathrm{S_{k0}}}, \breve{\mathbf{B}}_{\mathrm{S_{k1}}}), \tag{23}$$

$$\hat{\mathbf{c}} = [\overbrace{0,1,1,1,1}^{\tilde{n}=0}, 0, 1, 1, \cdots, \overbrace{0,1,1,1,1}^{\tilde{n}=2N_{\mathrm{s}}-1}]^{\mathrm{T}}, \tag{24}$$

$$\begin{aligned} \breve{\mathbf{G}}_{\mathrm{S_{km}}} &= (\hat{\mathbf{c}} \circ \tilde{\mathbf{w}}_{\mathrm{A}})^{\mathrm{H}} \hat{\mathbf{Q}}_{\mathrm{S_{km}}} (\hat{\mathbf{c}} \circ \tilde{\mathbf{w}}_{\mathrm{A}}), \\ \breve{\mathbf{B}}_{\mathrm{S_{km}}} &= (\hat{\mathbf{c}} \circ \tilde{\mathbf{w}}_{\mathrm{A}})^{\mathrm{H}} \hat{\mathbf{P}}_{\mathrm{S_{km}}} \tilde{\mathbf{I}}_1 (\hat{\mathbf{c}} \circ \tilde{\mathbf{w}}_{\mathrm{A}}), \end{aligned} \tag{25}$$

$$\hat{\mathbf{Q}}_{\mathrm{S_{k0}}} = \mathrm{diag}(\breve{\mathbf{Q}}_{\mathrm{S_{k0}}}, \mathbf{0}_{5\mathrm{N_s}}), \hat{\mathbf{Q}}_{\mathrm{S_{k1}}} = \mathrm{diag}(\mathbf{0}_{5\mathrm{N_s}}, \breve{\mathbf{Q}}_{\mathrm{S_{k1}}}), \tag{26}$$

$$\hat{\mathbf{P}}_{\mathrm{S_{k0}}} = \mathrm{diag}(\breve{\mathbf{P}}_{\mathrm{S_{k0}}}, \mathbf{0}_{5\mathrm{N_s}}), \hat{\mathbf{P}}_{\mathrm{S_{k1}}} = \mathrm{diag}(\mathbf{0}_{5\mathrm{N_s}}, \breve{\mathbf{P}}_{\mathrm{S_{k1}}}), \tag{27}$$

$$\begin{aligned} \breve{\mathbf{Q}}_{\mathrm{S_{km}}} &= \sum_{\theta \in \Theta_{\mathrm{s_k}}} \tilde{\mathbf{s}}_{\mathrm{m}}(\theta, \phi, \sigma, \eta) \tilde{\mathbf{s}}_{\mathrm{m}}(\theta, \phi, \sigma, \eta)^{\mathrm{T}}, \\ \breve{\mathbf{P}}_{\mathrm{S_{k0}}} &= \sum_{\theta \in \Theta_{\mathrm{s_k}}} \tilde{\mathbf{s}}_{0}(\theta, \phi, \sigma, \eta) \tilde{\mathbf{s}}_{1}(\theta, \phi, \sigma, \eta)^{\mathrm{T}}, \\ \breve{\mathbf{P}}_{\mathrm{S_{k1}}} &= \sum_{\theta \in \Theta_{\mathrm{s_k}}} \tilde{\mathbf{s}}_{1}(\theta, \phi, \sigma, \eta) \tilde{\mathbf{s}}_{0}(\theta, \phi, \sigma, \eta)^{\mathrm{T}}, \end{aligned} \tag{28}$$

where $\circ$ denotes the Hadamard product. Given the obtained $\tilde{\mathbf{w}}_{\mathrm{A}}$ in (21), to find $\mathbf{w}_{\mathrm{D}}$, the optimisation problem is given by

$$\min_{\mathbf{w}_{\mathrm{D}}} \quad \mathbf{w}_{\mathrm{D}}^{\mathrm{H}} \breve{\mathbf{M}}_{\mathrm{S}} \mathbf{w}_{\mathrm{D}}, \text{ subject to } \tilde{\mathbf{C}}^{\mathrm{H}} \mathbf{w}_{\mathrm{D}} = \mathbf{f}, \text{with} \tag{29}$$

$$\tilde{\mathbf{C}} = \begin{bmatrix} (\hat{\mathbf{c}} \circ \tilde{\mathbf{w}}_{\mathrm{A}})^{\mathrm{H}} \hat{\mathbf{z}}_{\mathrm{S_{00}}} & 0 \\ (\hat{\mathbf{c}} \circ \tilde{\mathbf{w}}_{\mathrm{A}})^{\mathrm{H}} \hat{\mathbf{z}}_{\mathrm{S_{01}}} & 0 \\ 0 & (\hat{\mathbf{c}} \circ \tilde{\mathbf{w}}_{\mathrm{A}})^{\mathrm{H}} \hat{\mathbf{z}}_{\mathrm{S_{10}}} \\ 0 & (\hat{\mathbf{c}} \circ \tilde{\mathbf{w}}_{\mathrm{A}})^{\mathrm{H}} \hat{\mathbf{z}}_{\mathrm{S_{11}}} \end{bmatrix}, \mathbf{f} = \begin{bmatrix} 1 \\ 1 \end{bmatrix}, \tag{30}$$

$$\hat{\mathbf{z}}_{\mathrm{S_{k0}}} = \begin{bmatrix} \breve{\mathbf{h}}_{\mathrm{k0}} \\ \mathbf{0}_{5\mathrm{N_s} \times 1} \end{bmatrix}, \hat{\mathbf{z}}_{\mathrm{S_{k1}}} = \begin{bmatrix} \mathbf{0}_{5\mathrm{N_s} \times 1} \\ \breve{\mathbf{h}}_{\mathrm{k1}} \end{bmatrix}, \tag{31}$$

$$\breve{\mathbf{h}}_{\mathrm{km}} = \sum_{\theta \in \Theta_{\mathrm{m_k}}} \begin{bmatrix} \mathbf{0} \\ \mathbf{s}_{\mathrm{m,x},0} \\ \mathbf{s}_{\mathrm{m,y},0} \\ -\Im(\mathbf{s}_{\mathrm{m,x},0}) + j\Re(\mathbf{s}_{\mathrm{m,x},0}) \\ -\Im(\mathbf{s}_{\mathrm{m,y},0}) + j\Re(\mathbf{s}_{\mathrm{m,y},0}) \\ \vdots \\ \mathbf{0} \\ \vdots \\ -\Im(\mathbf{s}_{\mathrm{m,y},N_s-1}) + j\Re(\mathbf{s}_{\mathrm{m,y},N_s-1}) \end{bmatrix}, \tag{32}$$

where $\mathbf{0}_{5\mathrm{N_s} \times 1}$ in (31) is a $5N_{\mathrm{s}} \times 1$ all-zero vector.

The solution to problem (29) is given by

$$\mathbf{w}_{\mathrm{D}} = \breve{\mathbf{M}}_{\mathrm{S}}^{-1} \tilde{\mathbf{C}} \left(\tilde{\mathbf{C}}^{\mathrm{H}} \breve{\mathbf{M}}_{\mathrm{S}}^{-1} \tilde{\mathbf{C}} \right)^{-1} \mathbf{f}. \tag{33}$$

Alternate optimisation of the digital coefficients $\mathbf{w}_{\mathrm{D}}$ and analogue coefficients $\tilde{\mathbf{w}}_{\mathrm{A}}$ can be achieved iteratively:

(1) First, via initialising the digital coefficients $\mathbf{w}_{\mathrm{D}}$ with random values, $\tilde{\mathbf{w}}_{\mathrm{A}}$ are obtained by substituting $a_{\mathrm{k,m}}(\{k, m\} \in \{0, 1\})$ into (12) or (21).
(2) Given the obtained optimum values for $\tilde{\mathbf{w}}_{\mathrm{A}}$ in step (1), the optimum values for $\mathbf{w}_{\mathrm{D}}$ are obtained by (33). Given the obtained values of $\mathbf{w}_{\mathrm{D}}$, the new set of values of $\tilde{\mathbf{w}}_{\mathrm{A}}$ can be obtained by (12) or (21) again.
(3) Repeat the step (2) until J_{LSE} in (12) or (21) converges.

IV. Design Examples

With $\phi = 90°$, the two beam directions are $\varphi_0 = -25°$ and $\varphi_1 = 15°$ and the sidelobe regions are $\Theta_{\mathrm{s}_0} \in [-90°, -35°] \cup [-15°, 90°]$ and $\Theta_{\mathrm{s}_1} \in [-90°, 5°] \cup [25°, 90°]$, sampled every $1°$. Antennas whose amplitude of weighting coefficients falls below 2×10^{-2} will be removed and the polarisation information is given by $\eta = 100°$ and $\sigma = 45°$.

The number of potential antennas for each subarray is $N_{\mathrm{s}} = 25$ and the adjacent antenna spacing is $d = \frac{\lambda}{3}$. The trade-off factor in (21) and (12) is $\alpha = 0.5$ and the zeroth and first beam responses generated by the whole antenna switch off method (21) and the dipole switched-off method (12) are displayed in Figs. 3 and 4, respectively.

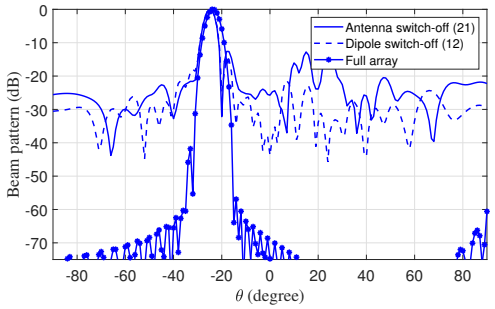

Fig. 3. Beam patterns of the zeroth beam with $\varphi_0 = -25°$.

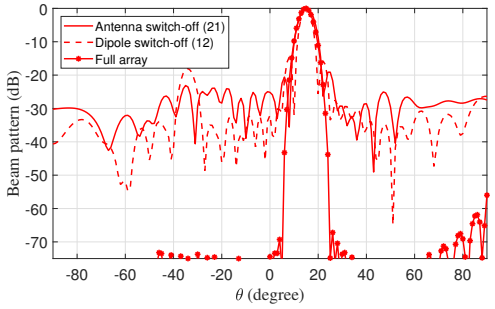

Fig. 4. Beam patterns of the first beam with $\varphi_1 = 15°$.

The numbers of resultant antennas for the antenna switch-off method (21) and the dipole switch-off method (12) are 33 and 36, respectively. However, if we count the total number of dipoles required, then it is 45 for (12), less than 66 for (21). As expected, due to the additional constraint introduced in (21), the sidelobe responses of the two beams generated by the proposed method (21) are higher than those of the dipole switch-off method (12), and the main beams are also a little wider. On the other hand, compared to the case using the full array, i.e., without any antennas/dipoles being switched off, the performance of both methods is not as good, with a much higher sidelobe level.

V. Conclusion

The optimum antenna selection problem for multi-beam multiplexing design based on crossed-dipole arrays has been studied from two different aspects: either choosing to switch off the individual dipoles of each crossed-dipole antenna or switch off the whole crossed-dipole antennas. Two designs have been developed and both work effectively with an overall reduced number of antennas/dipoles. However, the design based on switching off individual dipoles has provided a better result due to a relaxed constraint in its design.

References

[1] F. Boccardi, R. W. Heath, A. Lozano, T. L. Marzetta, and P. Popovski, "Five disruptive technology directions for 5G," *IEEE Commun. Mag.*, vol. 52, no. 2, pp. 74–80, Feb. 2014.

[2] Q. Luo, S. Gao, W. Liu, and C. Gu, *Low-cost Smart Antennas*, Wiley Press, Mar. 2019.

[3] W. Roh, J. Seol, J. Park, *et al.*, "Millimeter-wave beamforming as an enabling technology for 5G cellular communications: Theoretical feasibility and prototype results," *IEEE Commun. Mag.*, vol. 52, no. 2, pp. 106–113, Feb. 2014.

[4] S. Han, C. I. I, Z. Xu, and C. Rowell, "Large-scale antenna systems with hybrid analog and digital beamforming for millimeter wave 5G," *IEEE Commun. Mag.*, vol. 53, no. 1, pp. 186–194, Jan. 2015.

[5] A. F. Molisch, V. V. Ratnam, S. Han, Z. Li, S. L. H. Nguyen, L. Li, and K. Haneda, "Hybrid beamforming for massive MIMO: A survey," *IEEE Commun. Mag.*, vol. 55, no. 9, pp. 134–141, Sep. 2017.

[6] F. Sohrabi and W. Yu, "Hybrid analog and digital beamforming for mmWave OFDM large-scale antenna arrays," *IEEE J. Sel. Areas Commun.*, vol. 35, no. 7, pp. 1432–1443, Jul. 2017.

[7] S. A. Busari, K. M. S. Huq, S. Mumtaz, *et al.*, "Generalized hybrid beamforming for vehicular connectivity using THz massive MIMO," *IEEE Trans. Veh. Technol.*, vol. 68, no. 9, pp. 8372–8383, Sep. 2019.

[8] K. Satyanarayana, M. El-Hajjar, P. Kuo, A. Mourad, and L. Hanzo, "Hybrid beamforming design for full-duplex millimeter wave communication," *IEEE Trans. Veh. Technol.*, vol. 68, no. 2, pp. 1394–1404, Feb. 2019.

[9] S. Payami, M. Ghoraishi, M. Dianati, and M. Sellathurai, "Hybrid beamforming with a reduced number of phase shifters for massive MIMO systems," *IEEE Trans. Veh. Technol.*, vol. 67, no. 6, pp. 4843–4851, Jun. 2018.

[10] Z. Zheng and H. Gharavi, "Spectral and energy efficiencies of millimeter wave MIMO with configurable hybrid precoding," *IEEE Trans. Veh. Technol.*, vol. 68, no. 6, pp. 5732–5746, Jun. 2019.

[11] M. M. Molu, P. Xiao, M. Khalily, K. Cumanan, L. Zhang, and R. Tafazolli, "Low-complexity and robust hybrid beamforming design for multi-antenna communication systems," *IEEE Trans. Wireless Commun.*, vol. 17, no. 3, pp. 1445–1459, Mar. 2018.

[12] A. Li and C. Masouros, "Energy-efficient SWIPT: From fully digital to hybrid analog–digital beamforming," *IEEE Trans. Veh. Technol.*, vol. 67, no. 4, pp. 3390–3405, Apr. 2018.

[13] V. Venkateswaran and A. van der Veen, "Analog beamforming in MIMO communications with phase shift networks and online channel estimation," *IEEE Trans. Signal Process.*, vol. 58, no. 8, pp. 4131–4143, Aug. 2010.

[14] O. Oliaei, "A two-antenna low-IF beamforming MIMO receiver," in *Proc. IEEE Global Communications Conference*, Washington, DC, USA, Nov. 2007, pp. 3591–3595.

[15] C. Miller, W. Liu, and R. J. Langley, "Reduced complexity MIMO receiver with real-valued beamforming," in *Proc. IEEE International Conference on Computer and Information Technology*, Liverpool, UK, Oct. 2015, pp. 31–36.

[16] W. Liu and S. Weiss, *Wideband Beamforming: Concepts and Techniques*, John Wiley & Sons, Mar. 2010.

[17] X. Huang and Y. Guo, "Frequency-domain AoA estimation and beamforming with wideband hybrid arrays," *IEEE Trans. Wireless Commun.*, vol. 10, no. 8, pp. 2543–2553, Aug. 2011.

[18] J. A. Zhang, X. Huang, V. Dyadyuk, and Y. J. Guo, "Massive hybrid antenna array for millimeter-wave cellular communications," *IEEE Wirel. Commun.*, vol. 22, no. 1, pp. 79–87, Feb. 2015.

[19] Y. Guo, X. Huang, and V. Dyadyuk, "A hybrid adaptive antenna array for long-range mm-Wave communications," *IEEE Antennas Propag. Mag.*, vol. 54, no. 2, pp. 271–282, Apr. 2012.

[20] S. Fujio, C. Kojima, T. Shimura, *et al.*, "Robust beamforming method for SDMA with interleaved subarray hybrid beamforming," in *Proc. IEEE Annual International Symposium on Personal, Indoor, and Mobile Radio Communications (PIMRC)*, Valencia, Spain, Sep. 2016, pp. 1–5.

[21] T. Shimura, T. Ohshima, H. Ashida, *et al.*, "Millimeter-wave TX phased array with phase adjusting function between transmitters for hybrid beamforming with interleaved subarrays," in *Proc. European Microwave Conference (EuMC)*, London, UK, Oct. 2016, pp. 1572–1575.

[22] P. Rocca, R. Haupt, and A. Massa, "Sidelobe reduction through element phase control in uniform subarrayed array antennas," *IEEE Antennas Wireless Propag. Lett.*, vol. 8, pp. 437–440, Feb. 2009.

[23] Z. Li, A. Honda, T. Shimura, *et al.*, "Multi-user mmWave communication by interleaved beamforming with inter-subarray coding," in *Proc. IEEE Annual International Symposium on Personal, Indoor, and Mobile Radio Communications (PIMRC)*, Montreal, QC, Canada, Oct. 2017, pp. 1–6.

[24] M. Shimizu, "Millimeter-wave beam multiplexing method using subarray type hybrid beamforming of interleaved configuration with inter-subarray coding," *Int. J. Wirel. Inf. Netw.*, vol. 24, no. 3, pp. 217–224, Sep. 2017.

[25] J. Zhang, W. Liu, C. Gu, S. S. Gao, and Q. Luo, "Multi-beam multiplexing design for arbitrary directions based on the interleaved subarray architecture," *IEEE Trans. Veh. Technol.*, vol. 69, no. 10, pp. 11220–11232, Oct. 2020.

[26] X. Zhong, A. B. Premkumar, and H. Wang, "Multiple wideband acoustic source tracking in 3-D space using a distributed acoustic vector sensor array," *IEEE Sensors J.*, vol. 14, no. 8, pp. 2502–2513, Aug. 2014.

[27] M. Hawes, L. Mihaylova, and W. Liu, "Location and orientation optimization for spatially stretched tripole arrays based on compressive sensing," *IEEE Trans. Signal Process.*, vol. 65, no. 9, pp. 2411–2420, May 2017.

[28] G. Zhang, "A novel spatially spread electromagnetic vector sensor for high-accuracy 2-D DOA estimation," *Multidimens. Syst. Signal Process.*, vol. 28, May 2017.

[29] W. Yang, W. Xia, Z. He, and Y. Sun, "Polarimetric detection for vector-sensor processing in quaternion proper gaussian noises," *Multidimens. Syst. Signal Process.*, vol. 27, May 2015.

[30] J. Zhang and W. Liu, "Antenna selection for multi-beam multiplexing design based on the hybrid beamforming architecture," in *Proc. IEEE Statistical Signal Processing Workshop (SSP)*, Rio de Janeiro, Brazil, 2021, pp. 261–265.

[31] R. Compton, "The tripole antenna: An adaptive array with full polarization flexibility," *IEEE Trans. Antennas Propag.*, vol. 29, no. 6, pp. 944–952, Nov. 1981.

[32] B. Leprettre, N. Martin, F. Glangeaud, and J. -. Navarre, "Three-component signal recognition using time, time-frequency, and polarization information-application to seismic detection of avalanches," *IEEE Trans. Signal Process.*, vol. 46, no. 1, pp. 83–102, Jan. 1998.

[33] R. Bansal, "Tripole to the rescue [antennas]," *IEEE Antennas Propag. Mag.*, vol. 43, no. 2, pp. 106–107, Apr. 2001.

[34] K. T. Wong, "Blind beamforming/geolocation for wideband-FFHs with unknown hop-sequences," *IEEE Trans. Aerosp. Electron. Syst.*, vol. 37, no. 1, pp. 65–76, Jan. 2001.

[35] X. R. Zhang, Z. W. Liu, W. Liu, and Y. G. Xu, "Quasi-vector-cross-product based direction finding algorithm with a spatially stretched tripole"," in *Proc. IEEE TENCON Conference*, Xi'an, China, Oct. 2013.

[36] Y. Zhao, W. Liu, and R. J. Langley, "Adaptive wideband beamforming with frequency invariance constraints," *IEEE Trans. Antennas Propag.*, vol. 59, no. 4, pp. 1175–1184, Apr. 2011.

[37] M. Grant and S. Boyd, "CVX: Matlab software for disciplined convex programming, version 2.1," http://cvxr.com/cvx, Mar. 2014.

[38] M. Hawes and W. Liu, "Compressive sensing based design of sparse tripole arrays," *Sensors*, vol. 15, no. 12, pp. 31056–31068, 2015.